



Effect of deposition time on the optical properties of vanadium pentoxide films grown on porous silicon nanostructure

Skander Ktifa¹ · Mehdi Rahmani² · Mongi Bouaicha¹

Received: 25 September 2023 / Revised: 14 November 2023 / Accepted: 15 December 2023
© The Author(s) under exclusive licence to Associação Brasileira de Engenharia Química 2024

Abstract

Vanadium pentoxide (V_2O_5) thin films were grown on porous silicon (PS) layer by electron beam evaporation technique under an oxygen partial pressure. The morphology of the porous surface before and after V_2O_5 deposition for different evaporation times was observed by the Scanning Electron Microscope (SEM). The predicts changes of the chemical composition and bonds at the porous surface have been studied by FTIR and Raman spectroscopies. Photoluminescence (PL) spectroscopy was carried out to study the effect of vanadium pentoxide thickness on the optical properties of V_2O_5 /PS nanocomposites. The PL spectrum of PS show a red-shift of 90 nm following the deposition of vanadium pentoxide while a quenching of the PL intensity was observed. Referring to FTIR and Raman results, the origin of this shift can be attributed to the formation of oxidized vanadium elements at PS surface as well as the creation of localized states by V_2O_5 molecules inside the band gap of PS. The wavelength dependence of optical transmittance, reflectance and absorption coefficients were investigated. An increase in the optical band gap from 1.95 to 2.18 eV was obtained due to Moss-Burstein effect as well as the presence of vacancy defects in V_2O_5 film.

Keywords Porous silicon · Vanadium pentoxide · Photoluminescence · Optical band gap

Introduction

Over the last years, Vanadium pentoxide (V_2O_5) has received an important attention in research and technology. It is widely used for the development of electrical switching devices (Viswanathan et al. 2019), photodetector (Shafique et al. 2019), catalysts (Jin et al. 2011), optoelectronics (Yu et al. 2012), and sensors (Yan et al. 2015). In general, vanadium oxides are known by their diversified layered structures, wide bandgap, high chemical activity as well as its interesting optical and electrical properties (Mane et al. 2015; Abdel Maksoud et al. 2023). However, these properties strongly depend on the elaboration methods and proceedings used to prepare films. Vanadium pentoxide thin

films can be prepared on different substrates by a variety of deposition techniques like electron beam evaporation (Ramana et al. 1997), magnetron sputtering technique (Khairy et al. 2023), pulsed laser deposition (Julien et al. 1999), chemical deposition method (Nandakumar and Seebauer 2011) and sol-gel process (Jin et al. 2009). In other hand, porous silicon (PS) has attracted great attention with the discovery of its emission properties (Canham 1990). Since then, several studies were focused on the development of optic devices (Sharmila 2023), sensors (Arshavsky-Graham et al. 2019), medical applications (Tieu et al. 2019), solar cells (Rotshteyn et al. 2021), and waveguides (Escobar et al. 2018) using PS as base material. PS in the nanoporous regime with pore diameters from 2 to 5 nm has been known since 1990 by its emission of light in the visible range and it is still the subject of intense research (Canham 1990). In order to improve the optical performance and solve the problem of instability of the PS structure, several studies have focused on the deposition or the infiltration of certain chemical elements in the porous layer. Amdouni et al. (2015) have investigated the optical properties of SP/Ni composites prepared by electrodeposition method, they found a great enhancement in the integrated PL intensity of PS containing

✉ Skander Ktifa
ktifa.skander@gmail.com

¹ Laboratoire de Photovoltaïque, Centre de Recherches et des Technologies de L'Energie, Technopole de Borj-Cédria, B.P. 95, 2050 Hammam-Lif, Tunisia

² Laboratory of Nanomaterials, Nanotechnology and Energy, Department of Physics, Faculty of Sciences of Tunis, University of Tunis El Manar, 2092 El Manar, Tunis, Tunisia

nickel. Knowing that PL is an optical phenomenon which manifests itself by the emission of light by a material following the absorption of incident light whose energy is greater than its energy band gap. Thus, Ni elements contribute to the radiative recombination process which leads to an improvement in the optical properties of PS. Ktifa et al. (2018) have investigated the photothermal properties of PS/Rhodamine 6G nanocomposites. They found an enhancement in the thermal conduction and the PL emission by the insertion of Rhodamine molecules in the porous matrix. They reported that an energy transfer from PS to nanocomposite band can take place due to Rh6G. Due to the fact that the PS has a large specific surface area that can be modified with a wide variety of chemistry products and polymers. Recently, McInnes et al. (2021) have reported interesting properties of porous silicon-polymer composites and their applications in tissue engineering. In the present study, we report on V_2O_5 thin films deposited on PS with different thicknesses prepared by electron beam evaporation method. The vacuum evaporation technique can control the increase in layer thickness and minimize the level of impurity, which has an advantage over other deposition methods. We discuss the effect of V_2O_5 in morphological, optical, and room-temperature PL properties. V_2O_5 /PS/Si structure has been used to detect ethanol vapor at different concentrations by Chebout et al. (2013). Thanks to the electronic properties of V_2O_5 particles, conductance and capacitance measurements at low frequencies indicate the presence of interface states which can follow an alternating current signal that contributes to excess capacitance and conductance.

Our objective is to develop a selective layer of V_2O_5 capable of significantly increasing of the optical properties of PS. To achieve this goal, we have chosen the evaporation method which makes it possible to control the growth of the thin layers of V_2O_5 . The elaborated composites may be used as basic materials for several applications such as optoelectronics and photovoltaics.

Experimental

Porous Silicon (PS) was obtained using an electrochemical anodization etching method. P-type silicon substrates with (100) orientation, 20–50 Ω cm resistivity and cut into square-shaped pieces with an area of 1 cm^2 , were used as starting material. The etching process was performed using a Teflon cell where the substrates were placed on the bottom part facing upwards and in contact with an etching solution. The exposed area of the Si substrate was circular with a diameter of 0.9 cm. A platinum grid suspended in the etching solution was used as the cathode while the back side of the substrate itself was used as the anode. The samples were etched at room temperature using

a mixed solution containing HF (40%), ethanol and H_2O with the same volume proportions. The current density was fixed at 20 mA cm^{-2} and the etching time was taken 10 min. After etching, the samples were rinsed with ethanol and deionized water. The vanadium pentoxide (V_2O_5) layer was deposited on PS surface using a thermal evaporation system under vacuum conditions at the pressure of $4 \cdot 10^{-6}$ mbar. The deposition speed in the thermal evaporation method is set at 0.8 nm/s. The evaporation times were 250 s, 375 s and 500 s allowing to have layers with thicknesses of 200 nm, 300 nm and 400 nm, respectively. A schematic representation of the synthesis process has been illustrated in Fig. 1.

A Bruker DektakXT stylus profiler was used to take measurements of the V_2O_5 layer thicknesses. This profiler measures large vertical features of surfaces (up to 1 mm in height) with angstrom-level repeatability. The DektakXT uses Bruker's 64-bit parallel processing operating and analysis software, Vision64, which enables rapid data processing of large 3D map files. A confocal micro-Raman (Jobin–Yvon—T64000) with a resolution of 0.1 cm^{-1} and a recording time set at 30 s was used to perform Raman measurements. The morphologic observations of the synthesized composites were performed by using scanning electron microscope of ESEM Quanta 200 type of the FEI Company. The photoluminescence spectra were obtained using a GaAs photomultiplier combined with a standard lock-in technique and through a 220 mm Jobin–Yvon monochromator with a resolution of 0.2 nm. An argon laser source emitting at 488 nm wavelength was used as a light source excitation for both Raman and PL measurements. Fourier transform infrared (FTIR) spectra were recorded in 400–4000 cm^{-1} range with a step of 2 cm^{-1} in transmission mode using a Bruker IFS 66 V/S -type spectrometer (vacuum instrument). The optical data of transmittance and reflectance spectra are carried out by Perkin Elmer Lambda 950 spectrophotometer in 300–2000 nm wavelength range.

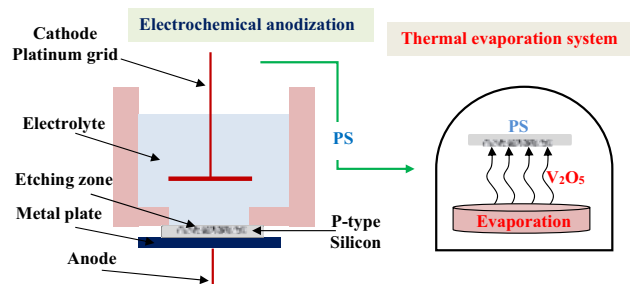


Fig. 1 Schematic illustration of the SP/ V_2O_5 nanocomposite synthesis process

Results and discussion

Firstly, we note that the elaboration conditions that we have adopted during the electrochemical etching process allow us to have a porous silicon (PS) layer with a porosity of 70 % and a thickness of 7 μm (Bessaïs et al. 2000; Bisi 2000).

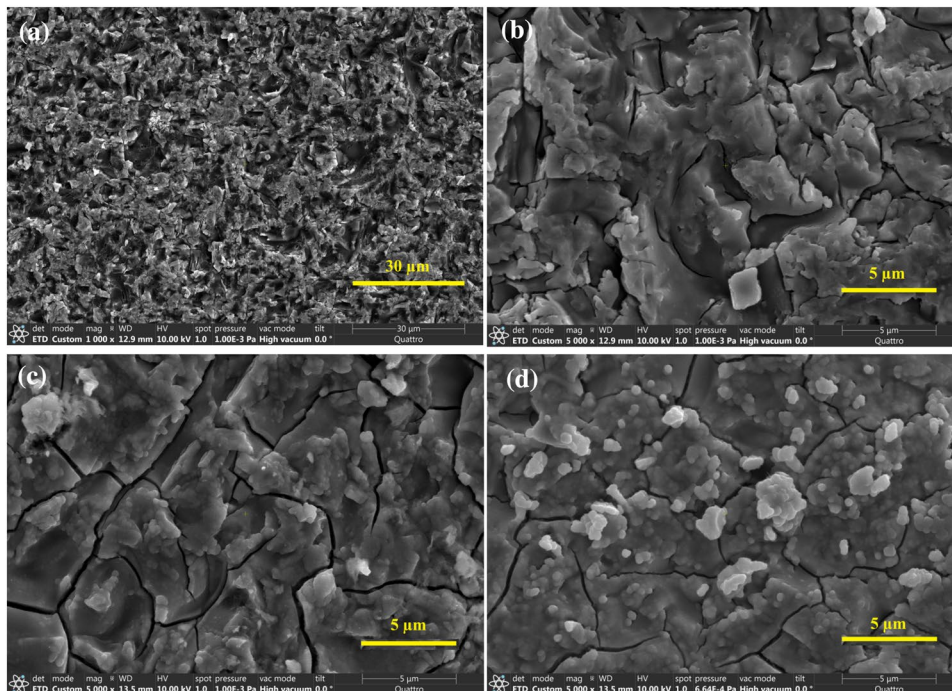
Knowing that the deposition speed in the thermal evaporation method is set at 0.8 nm/s and the evaporation times of V_2O_5 particles were 250 s, 375 s and 500 s. The estimated thicknesses of V_2O_5 layers are then 200 nm, 300 nm and 400 nm. To confirm these thickness values, we carried out measurements using the profilometer technique. The values (E_{prf}) found by this technique are very close to those estimated from the parameters taken in the evaporation process (E_{est}). The results of these measurements are given in Table 1.

Figure 2 shows plan view SEM images of porous silicon (PS) before treatment (a) and after deposition of V_2O_5 thin film with different thicknesses (200 nm (b), 300 nm (c), and 400 nm (d)). The SEM image in Fig. 2a shows a

Table 1 The thickness values found by the profilometer (E_{prf}) and those estimated from the parameters fixed in the evaporation process (E_{est})

t_{imm} (s)	250	375	500
E_{est} (nm)	200	300	400
E_{prf} (nm)	198.58	291.09	392.05

Fig. 2 Plan view SEM images of PS (a) and V_2O_5 thin film deposited onto PS with different thicknesses (200 nm (b), 300 nm (c), and 400 nm (d))



quasi-homogeneous and rough surface. The pores which appear as dark spots are distributed in the (100) plane thus forming a porous network on the silicon substrate. Images (b), (c) and (d) show remarkable changes in PS surface morphology after vanadium oxide evaporation. The surface morphology of V_2O_5 contains irregular nanoflakes interconnected to each other with the appearance of cracks and fissures on the outer surfaces with different lengths and orientations. A similar morphology containing cracks has been observed for layers of metal oxides such as iron oxide deposited on a PS matrix (Mabrouk et al. 2015). The presence of pores under the deposited layer promotes the formation of cracks across its surface leaving distinctive nanoflakes. These cracks form in a region of high stress related to defects in the crystal lattice. The decoration of V_2O_5 nanoflakes by light spots is shown on a $\text{SP}/\text{V}_2\text{O}_5$ surface with a thickness of 400 nm (Fig. 2d) with a strong synergy due to a large condensation and overaccumulation of vanadium oxide molecules.

We carried out measurements by FTIR spectroscopy on PS and $\text{PS}/\text{V}_2\text{O}_5$ nanocomposites with different thicknesses of V_2O_5 . The corresponding spectra are presented in Fig. 3 and the most distinguished peaks are numbered in this figure from 1 to 12.

The total number of peaks observed for the $\text{PS}/\text{V}_2\text{O}_5$ nanocomposites is greater than those in the PS spectrum which shows a direct effect of vanadium pentoxide deposition on the chemical composition at the porous surface. The strong absorption peaks numbered in the figure from 9 to 12 are attributed to the vibration modes of

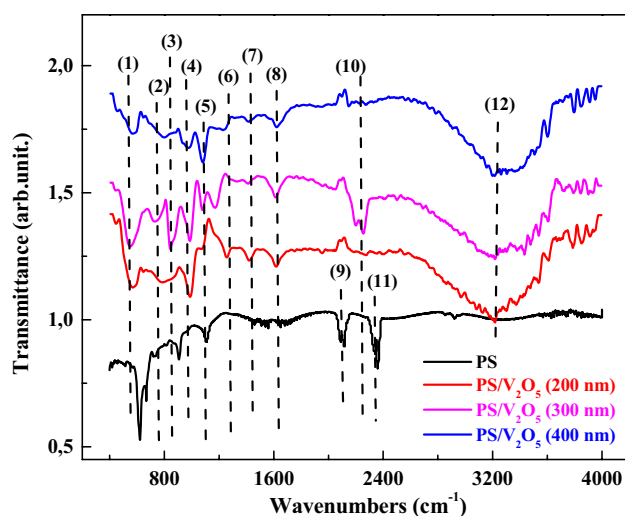


Fig. 3 FTIR spectra of PS and PS/V₂O₅ composites with different thicknesses of vanadium pentoxide layer

H₂O molecules and CH groups (Oktiani et al. 2019; Costa et al. 2012). The water molecules are localized inside the nanostructures coming from the etching solution following the electrochemical anodization process. The vibration band (N° 5) at 1060 cm⁻¹ corresponds to Si–O–Si and V=O terminal oxygen stretching mode (Jerbi et al. 2022; Baddour-Hadjean and Pereira-Ramos 2009). The band (N° 2) centered at around 760 cm⁻¹ is attributed to V–O–V asymmetric stretching mode (Jin et al. 2008).

The bonds formed by a triply coordinated oxygen atom between three vanadium atoms are also present at the porous surface, this is confirmed by the appearance of a vibration band (N° 1) at around 540 cm⁻¹ (Chu et al. 2016). The bands at 860 and 975 cm⁻¹ numbered by 3 and 4, which appear only for PS structures exposed to vanadium pentoxide evaporation, are attributed to non-bridging V–O bonds and the V=O stretching mode of the V–O axial bond, respectively (Frechero et al. 2007; Brown et al. 1989). The results obtained by FTIR spectroscopy show a high chemical reaction between V₂O₅ and PS surface. To confirm these observations, we carried out measurements by Raman spectroscopy. Figure 4 displays the Raman spectra of PS and PS/V₂O₅ nanocomposites recorded in the wavenumber range between 100 and 1100 cm⁻¹.

The main peak at 520 cm⁻¹ is the well-known first-order Raman scattering line of fundamental Si single crystal lattice vibrations. We note that the positions of the Raman vibration peaks of V₂O₅ change and shift depending on the matrix on which it is deposited. The peak at 995 cm⁻¹ corresponds to the vibration of V⁺⁵=O in stretching mode (Kang et al. 2012). A broad band which extends from 940 to 990 cm⁻¹ which becomes more intense by increasing the thickness of V₂O₅ showing an overlapping

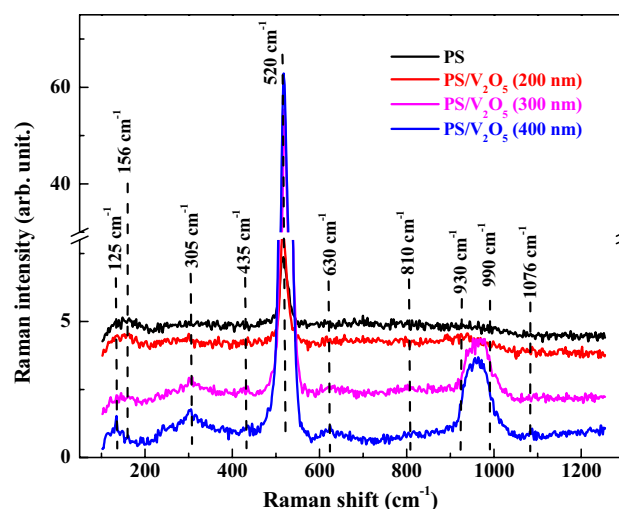


Fig. 4 Raman spectra of PS and PS/V₂O₅ composites with different thicknesses of vanadium pentoxide layer

of the vibrations of the Si–OH and V=O bonds (Meng et al. 2006).

The broad band at 305 cm⁻¹ is attributed to the bending vibrations of the triply coordinated oxygen (V₃-O) (Shvets et al. 2019). Two bands at 630 and 435 cm⁻¹, which appear clearly for relatively thick V₂O₅ layers, can be attributed to the vibrations of A_g phonons of VO₂ and the bending of VO₃, respectively (Meng et al. 2006; Frost et al. 2005). We note the appearance of certain vibration bands of low intensity at 810, 930 and 1076 cm⁻¹ which can be attributed to the vibrations of the V–O–V, V–O–Si and V=O bonds, respectively (Moisii et al. 2005). We also note that the vibration bands at 305 cm⁻¹, 630 cm⁻¹, 940 cm⁻¹ and 995 cm⁻¹ that appear in the PS/V₂O₅ spectrum have appeared in Raman spectra corresponding to silicon substrate in other work (Lee and Chang 2018). However, in our case, these vibration bands are very weak or absent in the Raman spectrum of the PS elaborated under the same conditions as those of the PS/V₂O₅. Nevertheless, they appear clearly in the spectra relating to PS/V₂O₅, this can be attributed to an enhancement of the Raman bands relating to the crystal lattice of Si caused by the Vanadium metal and it can also be explained by recrystallizing annealing of PS during the process of thermal evaporation.

The XRD diffraction patterns of V₂O₅ layers deposited onto PS substrate by electron beam evaporation method for different thicknesses are shown in Fig. 5. This figure shows the presence of diffraction peaks corresponding to V₂O₅ along different planes. The reflection peaks are sharp, suggesting high crystallinity of the PS/V₂O₅ nanocomposites. A predominant peak was observed in the XRD diffraction pattern at 60.8° which related with the preferred orientation along (701) plane. Furthermore, seven reflection peaks were

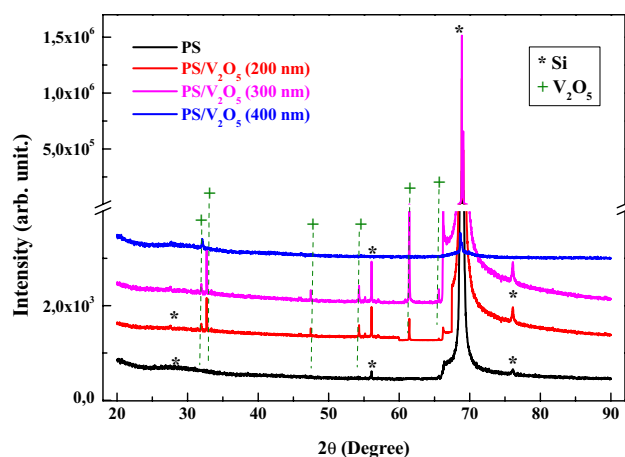


Fig. 5 XRD patterns of PS and PS/V₂O₅ for different thicknesses of vanadium pentoxide layer

observed at 2θ values of 31.5° , 32.8° , 47.6° , 54.3° , and 65.4° correspond to (310), (301), (600), (002), (012), and (711) reflections of the orthorhombic V₂O₅ material (Mu et al. 2015; Das et al. 2017).

The XRD peaks show the formation of high crystallinity orthorhombic phase of V₂O₅ which is similar to the results reported by several researchers (Schneider and Maziarz 2018; Govindarajan et al. 2019). The most intense peak for all patterns at 69.1° corresponds to the Si(400) (Rahmani et al. 2021a) while the peak at 51.2° is related to the diffraction from the p-type Si substrate (Ktifa and Rahmani 2023). We also note the presence of a broad band centered at 28.2° in the XRD pattern of PS indicating the presence of SiO₂ caused by a native oxidation (Rahmani et al. 2021b). This oxidation is reduced by the presence of V₂O₅ on the porous surface. No impurity peak was observed in XRD patterns of PS/V₂O₅ composites. Note also that there is an absence of certain diffraction peaks for a V₂O₅ layer with a thickness of 400 nm as well as a remarkable lowering of the intensity of the main peak at 69.1° . This is mainly due to the screening caused by the relatively large thickness of the V₂O₅ layer. XRD analysis results also confirmed the formation of PS/V₂O₅ composites.

In the light of SEM, FTIR, XRD and Raman results, we can conclude the establishment of chemical reactions between the porous surface and the V₂O₅ molecules. As it is known, V₂O₅ is an n-type semiconductor having a multiple valence range from V²⁺ to V⁵⁺, this can explain the variety of chemical bonds detected by FTIR and Raman spectroscopies.

Figure 6 shows the photoluminescence (PL) spectra of PS and PS/V₂O₅ with different thicknesses (200, 300 and 400 nm) under laser excitation fixed at 488 nm. PS exhibits the highest PL intensity. This is expected and is explained by the fact that the confinement of excitons in nanoporous silicon

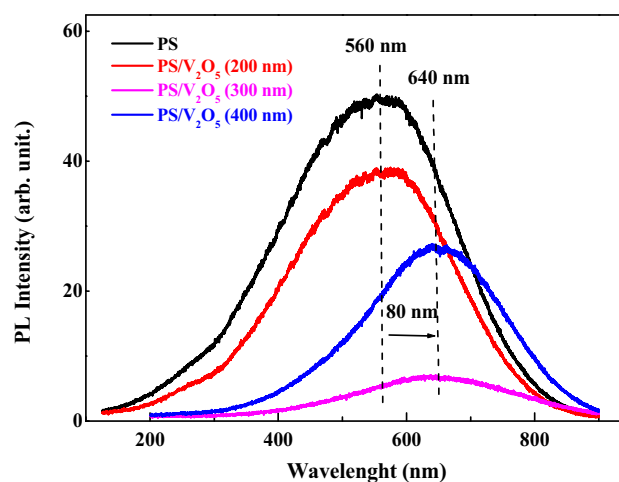


Fig. 6 PL spectra of PS and PS/V₂O₅ composites with different thicknesses of vanadium pentoxide layer

is very efficient in producing intense PL. When increasing the thickness of V₂O₅ thin films, PL shows a decrease of the peak intensity for 300 nm and then it increases and it remains lower than that of PS. The diffusion of vanadium oxide into the PS layer augments whenever increasing thickness thus influencing the porous structure which explains the dependence of the PL intensity with V₂O₅ deposition. Also, the density of non-radiative defects in the vanadium oxide layer is a determining factor in the emission efficiency obtained from these layers. This density is related to the thickness and the quantity of the V₂O₅ elements, this explains the lowering of the PL intensity compared to that of the PS. The quenching of the PL emission can be also due to the metal plasmonic absorption and non-radiative energy transfer due to vanadium deposition (Chalana et al. 2015). The PL peak position of PS/V₂O₅ with vanadium oxide thickness of 200 nm centered at 560 nm (2.21 eV) has not changed comparing it to that of PS before treatment, this is due to the band edge transition in V₂O₅ with a bandgap energy of 2.2–2.3 eV (Lamsal and Ravindra 2013). In the case of PS/V₂O₅ with 300 and 400 nm thickness, the PL band position is centered at 640 nm (1.94 eV), it therefore has a redshift of 80 nm. Given that the shift of the PL curves is essentially related to the crystallites size according to the quantum confinement model, the origin of the PL evolutions can be attributed to the increase in the concentration of oxygen atoms incorporated into the porous layer which affects the size of the oxidized silicon nanocrystals. The shift to lower energy could be also due to the trapped electrons at the located states related to Si–O bond of PS layer following the substitution of hydrogen atoms by oxygen as well as the oxide vanadium molecules V–O–V that are formed at PS surface according to the FTIR analysis (Ktifa et al. 2018; Rahmani et al. 2008). Moreover, the creation of intermediate

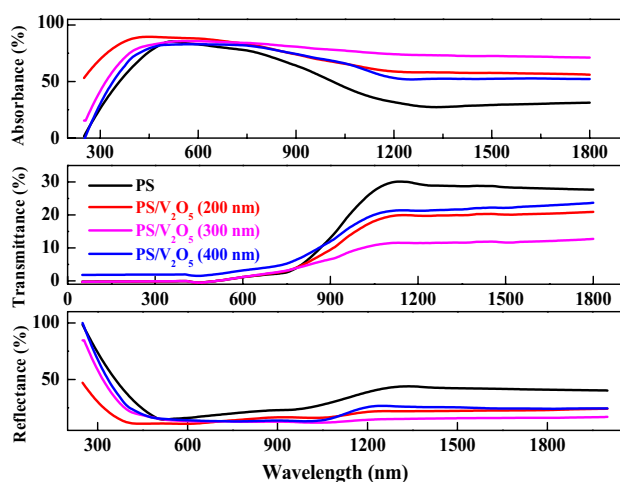


Fig. 7 UV-Vis-NIR absorbance, reflectance, and transmission spectra of PS and PS/V₂O₅ nanocomposite films for vanadium pentoxide thicknesses of 200, 300 and 400 nm

states by V₂O₅ inside the band gap of PS and the passage of the radiative recombinations through these levels is the cause of the redshift of the porous silicon PL curve.

Figure 7 displays the optical transmittance (T), reflectance (R), and absorbance (A) spectra of PS and PS/V₂O₅ with different thicknesses of V₂O₅ layer. The results obtained for each sample show a similar pattern. All samples show significant absorbance in the visible range, while reflectance and transmission are very low.

A similar optical behavior was found for different series of V₂O₅ thin layers (Schneider 2020). For absorbance spectra, a stability is observed in the entire visible range which extends up to 750 nm. In the N-IR region, unlike the PS/V₂O₅ composites, the absorbance decreases rapidly for the PS while the reflectance and the transmittance start increasing. It can also be seen that the transmittance percentage decreases as the thickness is increased. The absorption edge of the V₂O₅ grown film shifts to high energies and it was observed at a wavelength of approximately 1100 nm, and above the absorption edge, the transmittance decreased slightly with increasing wavelength from about 30% at 1100 nm to 10% at 1800 nm. The effect of vanadium oxide on the optical spectra manifests itself in the N-IR range. Indeed, a reduction in the transmission and reflectance percentages of about 20% and 25%, respectively. This percentage increases by about 40% for the absorbance by comparing the PS/V₂O₅ (300 nm) to the untreated PS.

The optical absorption coefficient is calculated by using the Beer – Lambert equation (Mäntele and Deniz 2017):

$$A = -\log(T) \quad (1)$$

Knowing that an accurate determination of the bandgap energy (E_g) is necessary to well understand the photophysical properties of semiconductor materials. In our study, we have used the Tauc method to determine the E_g values from optical spectra (Tauc et al. 1966). For excitation energies higher than gap energy, the quantity $(\alpha E)^n$ should have linear variations with E , following the Tauc law:

$$(\alpha E)^n = \beta(E - E_g) \quad (2)$$

where α is the absorption coefficient ($\alpha = A/L$ with L is the optic length), β is a constant related to the order in crystalline structure of deposited films, known as band edge sharpness. n can take the following values (1/2, 3/2, 2 or 3) according to the electronic structure of the material and the type of the dominant transitions. In the case of V₂O₅ thin film, $n = 1/2$ corresponding to an indirect allowed transition. By adopting this value of n , the curves of $(\alpha E)^{1/2}$ versus E are plotted and they are shown in Fig. 8. β is the slope of the straight line.

We can determine the energy band gap from the linear part by extrapolating the straight line until its intersection with the x-axis. An increased optical band gap from 1.95 eV to 2.18 eV was found by the deposition of a vanadium pentoxide layer. This increase is due to the Moss-Burstein effect (Dutta et al. 2021). Indeed, the V₂O₅ allows to inject carriers into the conduction band of PS, the Moss-Burstein effect occurs when the electron carrier concentration exceeds the conduction band.

Based on the above discussion and by referring to studies made on similar structures (Wang et al. 2019), a possible carrier transfer represented by electron transition/migration from V₂O₅ to PS may occur. We also note that following these surface modifications and the establishment of a V₂O₅/

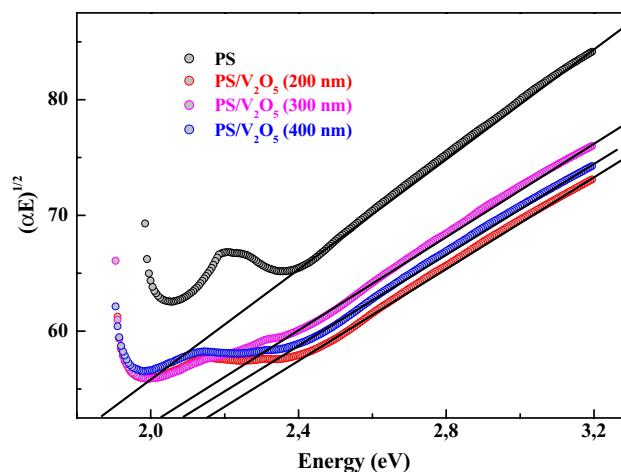


Fig. 8 $(\alpha E)^{1/2}$ versus energy E near the band gap for PS and PS/V₂O₅ with different thicknesses of V₂O₅

PS heterojunction, we obtained major changes in the optical properties. The same behavior is found for similar structures (Bento et al. 2023). The increase of the band gap can be also explained by the presence of vacancy defects in the V_2O_5 layer. These defects, induced by the vanadium pentoxide deposition and influenced by the variation in its thickness, affects the optical transitions and it is traduced by a PL shift as well as by a variation of the optical gap energy.

Conclusion

V_2O_5 thin films were fabricated on porous silicon by an environmentally friendly method. The results revealed that V_2O_5 thickness strongly affects the structure as well as the optical properties of the PS/ V_2O_5 nanocomposites. Photoluminescence spectra are red-shifted with the V_2O_5 layer thickness increases. In correlation with Raman and FTIR results, the observed PL shift is attributed to the trapped electrons at the located states owing to Si–O bond of PS layer and the oxidized Vanadium V–O–V molecules. A quenching of the PL emission is observed which can be due to the metal plasmonic absorption and non-radiative energy transfer due to vanadium deposition. Transmission, absorbance, and reflectance spectra changed with the variation of V_2O_5 thickness. The edge absorbance shifts to high energies due to the growth process leading to a variation in V_2O_5 thickness. Due to the presence of vacancy defects, the optical band gap increased from 1.95 to 2.18 eV after V_2O_5 deposition on porous matrix. The presence of vanadium pentoxide layer on PS offers the possibility to change and control the band gap energy. After deposition of V_2O_5 on its surface, the optical bandgap value of PS is within the desirable energy range for applications in photovoltaic solar cells. In the light of these results, PS/ V_2O_5 can be considered as a promising material for solar cells and optical switching device applications. As a perspective, we plan to study the electrical and photothermal properties of this material in future work.

Acknowledgements The authors would like to thank Dr. Jamila Bennaceur and Pr. Wissem Dimassi (Laboratoire de photovoltaïque et de semi-conducteurs, centre de recherche et de technologie de l'énergie, Hammam Lif— Tunisia) for FTIR measurements.

Authors contribution SK: Investigation, Data curation, Formal analysis, Writing— original draft. MR: Methodology, Validation, Writing— review & editing. MB: Supervision.

Data Availability Data will be made available on request.

Declarations

Conflict of interest The authors declare that they have no known competing financial interests or personal relationships that could have appeared to influence the work reported in this paper.

References

- Abdel Maksoud MIA, Fahim RA, Kassem SM, Awed AS (2023) Gamma irradiation-induced changes in structural, linear/nonlinear optical, and optoelectrical properties of PVB/BiVO₄ nanocomposite for organic electronic devices. *Opt Quant Electron* 55:1165
- Amdouni S, Rahmani M, Zaïbi M-A, Oueslati M (2015) Enhancement of Porous Silicon Photoluminescence by Electroless Deposition of Nickel 157:93–97
- Arshavsky-Graham S, Massad-Ivanir N, Segal E, Weiss S (2019) Porous silicon-based photonic biosensors: current status and emerging applications. *Anal Chem* 91:441–467
- Baddour-Hadjean R, Pereira-Ramos J-P (2009) Raman microspectrometry applied to the study of electrode materials for lithium batteries. *Chem Rev* 110:1278–1319
- R.T. Bento, O.V. Correa, P.L. Gastelois & M.F. Pillis, VIS-active TiO₂ films decorated by expanded graphite: impact of the exfoliation time on the photocatalytic behaviour, *Environmental Technology* 2023, 1–12
- Bessaïs B, Ben Younes O, Ezzaouia H, Mliki N, Boujmil MF, Oueslati M, Bennaceur R (2000) Morphological changes in porous silicon nanostructures: non-conventional photoluminescence shifts and correlation with optical absorption. *J Luminescenc* 90:101–109
- Bisi O (2000) Stefano Ossicini, L. Pavesi, Porous Silicon: a Quantum Sponge Structure for Silicon Based Optoelectronics, *Surface Science Reports* 38:1–126
- Brown DA, Glass WK, McGardle S (1989) Spectroscopic studies of vanadium complexes of benzohydroxamic acid. *Proc R Irish Acad Sect b: Biol Geol Chem Sci* 89:383–387
- Canham LT (1990) Silicon quantum wire array fabrication by electrochemical and chemical dissolution of wafers. *Appl Phys Lett* 57:1046–1048
- S. R. Chalana, V. Ganesan, and V. P. Mahadevan Pillai, Surface plasmon resonance in nanostructured Ag incorporated ZnS films, *AIP Advances* 2015, 5 ,107207.
- Chebout K, Iratni A, Bouremana A, Sam S, Keffous A, Gabouze N (2013) Electrical characterization of ethanol sensing device based on Vanadium oxide/Porous Si/Si structure. *Solid State Ionics* 253:164–168
- Chu J, Kong Z, Lu D, Zhang W, Wang X, Yu Y, Li S, Wang X, Xiong S, Ma J (2016) Hydrothermal synthesis of vanadium oxide nanorods and their electrochromic performance. *Mater Lett* 166:179–182
- Costa C, Pinheiro C, Henriques I, Laia CAT (2012) Inkjet printing of sol–gel synthesized hydrated tungsten oxide nanoparticles for flexible electrochromic devices. *ACS Appl Mater Interfaces* 4:5266–5275
- Das AS, Roy M, Roy D, Kar T, Rath S, Bhattacharya S (2017) Investigations of Microstructure and Dc Conductivity of V_2O_5 -Nd₂O₃ Glass Nanocomposites. *ChemistrySelect* 2:11273–11280
- M. Dutta, J.M. Kalita, G. Wary, Optical processes and apparent increase of optical band gap in Y₂O₃:Eu²⁺ nanoparticles synthesised by a gradually-heated solution combustion method 2021, 240, 166946.
- Escobar S, Nava R, Flores-Romero E, Reyes-Esqueda JA (2018) Light polarization in active photonic waveguides of porous silicon. *Photon Nanostruct Fundam Appl* 31:44–51
- Frechero MA, Quinzani OV, Pettigrosso RS, Villar M, Montani RA (2007) IR absorption spectra of lithium and silver vanadium–tellurite based glasses. *J Non-Cryst Solids* 353:2919–2925
- Frost RL, Erickson KL, Weier ML, Carmody O (2005) Raman and infrared spectroscopy of selected vanadates. *Spectrochimica Acta Part A* 61:829–834
- D. Govindarajan, V. Uma Shankar, R. Gopalakrishnan, Supercapacitor behavior and characterization of RGO anchored V_2O_5

- nanorods, *Journal of Materials Science: Materials in Electronics* 2019, 30, 16142–16155.
- Jerbi L, Rahmani M, Ajlani H, Guendouz M, Lorrain N, Oueslati M, Meftah A (2022) Highly improved optical properties of silicon nanowires by deposition of Poly[2-methoxy-5-(2'-ethylhexyloxy)-1,4-phenylene vinylene] polymer. *J Lumin* 244:118744
- Jin A, Chen W, Zhu Q, Yang Y, Volkov VL, Zakharova GS (2008) Electrical and electrochemical characterization of poly (ethylene oxide)/V₂O₅ xerogel electrochromic films. *Solid State Ionics* 179:1256–1262
- Jin A, Chen W, Zhu Q, Yang Y, Volkov VL, Zakharova GS (2009) Structural and electrochromic properties of molybdenum doped vanadium pentoxide thin films by sol-gel and hydrothermal synthesis. *Thin Solid Films* 517:2023–2028
- Jin W, Chen W, Lu Y, Zhao C, Dai Y (2011) V₂O₅/polypyrrole core-shell nanotubes for gas sensor. *J Nanosci Nanotechnol* 11:10834–10838
- Julien C, Haro-Poniatowski E, Camacho-López MA, Escobar-Alarcón L, J. Jimenez-Jarquín, (1999) Growth of V₂O₅ thin films by pulsed laser deposition and their applications in lithium micro-batteries. *Mater Sci Eng, B* 65:170–176
- Kang M, Oh E, Kim I, Kim SW, Ryu J-W, Kim Y-G (2012) Optical characteristics of amorphous V₂O₅ thin films colored by an excimer laser. *Curr Appl Phys* 12:489–493
- Khairy KT, Song Y, Yoon J-H, Montero J, Österlund L, Kim S, Song P (2023) Thermochromic properties of vanadium oxide thin films prepared by reactive magnetron sputtering at different oxygen concentrations. *Vacuum* 210:111887
- Ktifa S, Rahmani M (2023) Strong enhancement of the optical properties of SiNWs by the deposition of snowball-like V₂O₅ nanoparticles. *Opt Mater* 142:114144
- Ktifa S, Znaidi M, Saadallah F, Yacoubi N, Ezzaouia H (2018) Photo-thermal investigation of nanocomposite porous silicon / Rhodamine 6G. *SILICON* 10:1573–1577
- Lamsal C, Ravindra NM (2013) Optical properties of vanadium oxides-an analysis. *J Mater Sci* 48:634
- Lee W-J, Chang Y-H (2018) Growth without Postannealing of Monoclinic VO₂ Thin Film by Atomic Layer Deposition Using VCl₄ as Precursor. *Coatings* 8:431
- Mabrouk A, Lorrain N, Haji LM, Oueslati M (2015) Correlation between optical properties surface morphology of porous silicon electrodeposited by Fe³⁺ ion. *Superlatt Microstruct* 77:219–231
- Mane AA, Ganbavle VV, Gaikwad MA, Nikam SS, Rajpure KY, Moholkar AV (2015) Physicochemical properties of sprayed V₂O₅ thin films: Effect of substrate temperature. *J Anal Appl Pyrolysis* 115:57–65
- Mäntele W, Deniz E (2017) UV–VIS absorption spectroscopy: Lambert-Beer reloaded. *Spectrochim Acta Part A Mol Biomol Spectrosc* 173:965–968
- S.J.P. McInnes, R.B. Vasani, N.K. McMillan, N.H. Voelcker, Chapter 14 - Porous silicon-polymer composites for cell culture and tissue engineering, *Porous Silicon for Biomedical Applications (Second Edition)* Woodhead Publishing Series in Biomaterials 2021, 447–492.
- Meng L-J, Silva RA, Cui H-N, Teixeira V, Dos Santos M, Xu Z (2006) Optical and structural properties of vanadium pentoxide films prepared by dc reactivemagnetron sputtering. *Thin Solid Films* 515:195–200
- Moisii C, Curran MD, van de Burgt LJ, Stiegman AE (2005) Raman spectroscopy of discrete silica supported vanadium oxide: assignment of fundamental stretching modes. *J Mater Chem* 15:3519–3524
- Mu J, Wang J, Hao J, Cao P, Zhao S, Zeng W, Miao B, Xu S (2015) Hydrothermal synthesis and electrochemical properties of V₂O₅ nanomaterials with different dimensions. *Ceram Int* 41:12626–12632
- Nandakumar NK, Seebauer EG (2011) Low temperature chemical vapor deposition of nanocrystalline V₂O₅ thin films. *Thin Solid Films* 519:3663–3668
- Oktiani R, Ragadhita R, Nandiyanto ABD (2019) How to read and interpret FTIR spectroscopy of organic material. *Indonesian J Sci Technol* 4:97–118
- Rahmani M, Moadhen A, Zaïbi M-A, Elhouichet H, Oueslati M (2008) Photoluminescence enhancement and stabilisation of porous silicon passivated by iron. *J Lumin* 128:1763–1766
- Rahmani M, Amdouni S, Zaïbi MA, Meftah A (2021a) Temperature and Excitation Power Dependence of Photoluminescence and Electrical Characterization of Ni-Passivated Porous Silicon *Journal of Materials Science: Materials in Electronic* 32:4321–4330
- Rahmani M, Amdouni S, Zaïbi MA, Meftah A (2021b) Effect of etching duration on the morphological and opto-electrical properties of silicon nanowires obtained by Ag-assisted chemical etching. *SILICON* 13:179–187
- Ramana CV, Hussain OM, Naidu BS, Reddy PR (1997) Spectroscopic characterization of electron-beam evaporated V₂O₅ thin films. *Thin Solid Films* 305:219–226
- Rotshteyn VM, Turdaliev TK, Ashurov KhB (2021) On the question of the possibility of using nanocrystalline porous silicon in silicon-based solar cells. *Appl Solar Energy* 57:480–485
- Schneider K (2020) Optical properties and electronic structure of V₂O₅, V₂O₃ and VO₂. *J Mater Sci: Mater Electron* 1:10478–10488
- Schneider K, Maziarz W₂O₅ Thin Films as Nitrogen Dioxide Sensors *Proceedings* 2018, 2, 759.
- Shafique S, Yang S, Wang Y, Woldu YT, Cheng B, Ji P (2019) High-performance photodetector using urchin-like hollow spheres of vanadium pentoxide network device. *Sensors Actuators A* 296:38–44
- Sharmila B (2023) Ashutosh Kumar Dikshit, Priyanka Dwivedi, Role of etching parameters on the performance of porous silicon based photodetector devices. *Microelectron J* 140:105940
- Shvets P, Dikaya O, Maksimova K, Goikhman A (2019) A review of Raman spectroscopy of vanadium oxides. *J Raman Spectrosc* 50:1226–1244
- Tauc J, Grigorovici R, Vancu A (1966) Optical properties and electronic structure of amorphous Germanium. *Physica Status Solidi (b)* 15:627–637
- Tieu T, Alba M, Elnathan R, Cifuentes-Rius A, Voelcker NH (2019) Advances in porous silicon-based nanomaterials for diagnostic and therapeutic applications. *Adv Ther* 2:1800095
- Viswanathan A, Prakashaiah BG, Subburaj V, Shetty AN (2019) High energy reduced graphene oxide/vanadium Pentoxide/polyaniline hybrid supercapacitor for power backup and switched capacitor converters. *J Colloid Interface Sci* 545:82–93
- Wang C-C, Chen K-C, Shieu F-S, Shih HC (2019) Characterization and photoluminescence of V₂O₅@Pt core-shell nanostructures as fabricated by atomic layer deposition. *Chem Phys Lett* 729:24–29
- Yan W, Hu M, Wang D, Li C (2015) Room temperature gas sensing properties of porous silicon/V₂O₅ nanorods composite. *Appl Surf Sci* 346:216–222
- Yu M, Liu X, Wang Y, Zheng Y, Zhang J, Li M, Lan W, Su Q (2012) Gas sensing properties of p-type semiconducting vanadium oxide nanotubes. *Appl Surf Sci* 258:9554–9558

Publisher's Note Springer Nature remains neutral with regard to jurisdictional claims in published maps and institutional affiliations.

Springer Nature or its licensor (e.g. a society or other partner) holds exclusive rights to this article under a publishing agreement with the author(s) or other rightsholder(s); author self-archiving of the accepted manuscript version of this article is solely governed by the terms of such publishing agreement and applicable law.